Materials Science and Engineering A 532 (2012) 106–110

Contents lists available at SciVerse ScienceDirect

Materials Science and Engineering A

journal homepage: www.elsevier.com/locate/msea

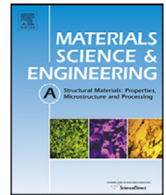

High tensile ductility via enhanced strain hardening in ultrafine-grained Cu

P. Xue, B.L. Xiao, Z.Y. Ma*

Shenyang National Laboratory for Materials Science, Institute of Metal Research, Chinese Academy of Sciences, 72 Wenhua Road, Shenyang 110016, China

ARTICLE INFO

Article history:
Received 29 July 2011
Received in revised form 11 October 2011
Accepted 12 October 2011
Available online 25 October 2011

Keywords:
Copper
Grain boundaries
Ductility
Dynamic recrystallization
Friction stir processing

ABSTRACT

Low tensile ductility owing to the insufficient strain hardening is the main drawback for ultrafine-grained (UFG) materials, which restricts their practical applications. Here, via a simple friction stir processing technique with additional cooling, we prepared UFG Cu with high strength and tensile ductility. Enhanced strain hardening capacity, which is effective in blocking and accumulating dislocations, was achieved in the present recrystallized UFG microstructure. The enhanced strain hardening capacity is attributed primarily to the low dislocation density, and the presence of large fraction of high angle grain boundaries and a certain amount of coherent twin boundaries. This work provides a strategy for designing UFG materials with good mechanical properties.

© 2011 Elsevier B.V. All rights reserved.

1. Introduction

Good matching of strength and ductility for structure materials has been a long-standing mission for material scientists. Significant increases in hardness and strength have been documented for nanostructured and ultrafine-grained (UFG) materials [1]. Disappointingly, nearly all these metals have low tensile ductility at ambient temperature, which limits their practical applications. The elongation to failure is far less than that of their coarse-grained counterpart. More importantly, the useful uniform tensile deformation, i.e. the plastic strain before localized deformation, is close to zero for almost all UFG and nanostructured materials [2–4].

The disappointingly low ductility can be attributed to the artifacts from processing, the plastic instability with little or no strain hardening (dislocation storage) capacity, and low resistance to crack initiation and propagation [3]. Recently, a variety of strategies aimed at improving the poor ductility of the UFG and nanostructured materials have been reported [5–9]. Despite varying degrees of success, most of these strategies have inherent processing and/or material limitations. Preparing UFG and nanostructured materials with sound mechanical properties using simple processing methods is still a technical challenge.

One-step severe plastic deformation (SPD) provides practical approaches to producing 100% dense bulk UFG materials that can exhibit mechanical properties controlled by their intrinsic deformation mechanisms [10]. However, even these UFG materials always exhibit a low tensile ductility owing to their insufficient strain hardening capacity [11–14]. Recently, a new simple processing technique – friction stir processing (FSP), was developed by Mishra et al. [15] for microstructral modification, based on the basic principles of friction stir welding. FSP causes intense plastic deformation, densification, and homogeneity of the processed zone, thereby changing the mechanical properties [15,16].

Moreover, FSP is also an effective method of preparing bulk UFG materials, such as aluminum and magnesium alloys [17–20]. After FSP, the microstructure of the processed zone is characterized by equiaxed dynamically recrystallized grains with large fraction of high angle grain boundaries (HAGBs, misorientation angle >15°) and low density of dislocations [15–20]. This is quite different from most other plastically deformed UFG microstructures originating from the dislocation related mechanism [11–14].

Recently, Zhao et al. [8] summarized the developed strategies to improve the ductility of the UFG materials, and pointed out that increasing the fraction of HAGBs and decreasing the dislocation density were effective methods of improving the ductility of the UFG pure metals. Considering that the FSP materials generally have low density of dislocations and large fraction of HAGBs, it is worthwhile to investigate whether the enhanced tensile ductility can be achieved in the FSP UFG materials. In this study, UFG Cu was produced via FSP at low heat input, and the microstructure and tensile properties of the UFG Cu were examined. The purpose is to achieve an ideal combination of high strength and enhanced ductility.

2. Experimental procedures

In order to investigate the intrinsic deformation mechanism, we used the high pure (99.99%) oxygen free Cu as our target metal.

* Corresponding author. Tel.: +86 24 83978908; fax: +86 24 83978908.
E-mail address: zyma@imr.ac.cn (Z.Y. Ma).

0921-5093/$ – see front matter © 2011 Elsevier B.V. All rights reserved.
doi:10.1016/j.msea.2011.10.070

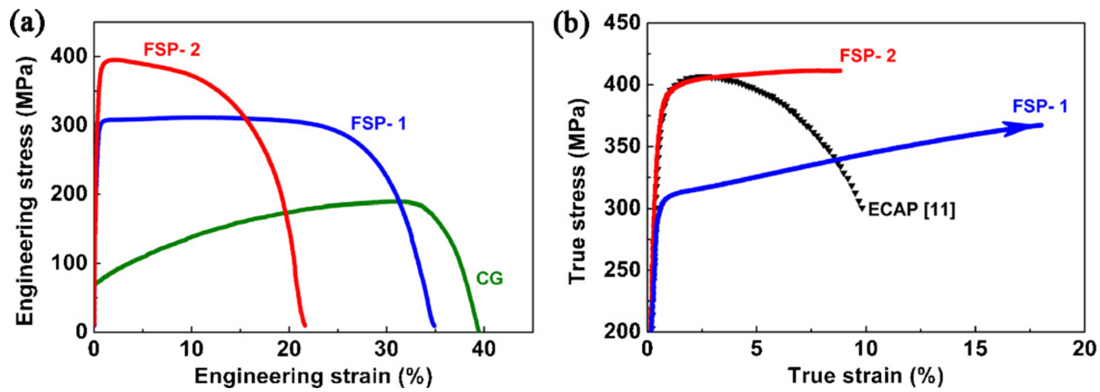

Fig. 1. (a) Tensile engineering stress–strain curves of FSP Cu and CG Cu samples and (b) true stress–strain curves of FSP Cu and 16-passes ECAP Cu [11].

To yield low heat-input, two pure Cu plates (designated as FSP-1, FSP-2, respectively) were first fixed in water. During FSP, additional cooling by the flowing water was adopted. The water flew out from the 4 mm diameter outlet at a velocity of about 7 L/min. The FSP-1 Cu sample was prepared using a rotating tool with a shoulder 12 mm in diameter at a rotation rate of 600 rpm and a traverse speed of 50 mm/min, whereas the FSP-2 Cu sample was processed using a smaller tool shoulder 8 mm in diameter at a processing parameter of 400 rpm – 50 mm/min.

For the tensile test, the dog-bone-shaped tensile specimens with a gauge length of 5 mm and a width of 1.2 mm were machined along the processing direction from the processed zone, and polished to a thickness of 0.6 mm. Uniaxial tensile tests were conducted at room temperature at an initial strain rate of $1 \times 10^{-3}\ s^{-1}$. After tensile tests, the fracture surfaces of the samples were examined on a scanning electron microscope (SEM, Quanta 600).

Microstructural examination was completed with SEM, transmission electron microscopy (TEM) and electron backscatter diffraction (EBSD). TEM observation was carried out on a FEI Tecnai G^2 20 microscope operating at 200 kV. Thin foils for TEM were twin-jet electropolished by a solution (25% alcohol, 25% phosphorus acid and 50% deionized water) at 263 K. EBSD scans were performed using an Oxford HKL Channel 5 system on a LEO Supra 35 FEG SEM with step size of 70 nm.

3. Results and discussion

The engineering tensile stress–strain curves of the FSP Cu samples, as well as the coarse grained (CG) Cu reference material, are compared in Fig. 1a. The CG Cu exhibited a low yield strength of ~60 MPa and an elongation of ~40%. It is apparent that under an appropriate heat-input, the FSP-1 Cu sample showed a very large elongation of ~35% with a high yield strength near 300 MPa. More importantly, the FSP-1 Cu sample exhibited a considerable uniform elongation of ~10%. When the heat-input was lower during FSP, the FSP-2 Cu sample showed a higher yield strength of ~370 MPa with an elongation to failure of ~22%. The fact that both FSP Cu samples showed high tensile ductility suggests that the fast plastic instability observed in most UFG materials was restrained in the present FSP Cu samples. This should be attributed to the regaining of the strain hardening capacity in the FSP Cu samples, which can be observed from the true stress–strain curve (Fig. 1b).

It is obvious that the stress of the 16-pass equal channel angular processed (ECAP) Cu sample decreased quickly after a small plastic strain (~2%) [11]. However, the FSP Cu samples showed a continuous strain hardening to significant strains, resulting in the high tensile ductility. This difference is further verified by the normalized strain hardening rate Θ versus the true strain curve as shown in Fig. 2. The normalized strain hardening rate Θ was defined as

$$\Theta = \frac{1}{\sigma}\left(\frac{\partial\sigma}{\partial\varepsilon}\right)_{\dot{\varepsilon}} \quad (1)$$

where σ and ε are the true stress and true strain, respectively. Fig. 2 demonstrates that the FSP-1 sample exhibited positive strain hardening to significant strains compared to that of the SPD samples. The enhanced strain hardening capacity of the FSP Cu samples is controlled by their microstructures. In the following paragraphs, the microstructures of the FSP Cu samples are analyzed in detail to identify the mechanism responsible for the enhanced strain hardening capacity.

Fig. 3 shows the TEM bright-field images of the FSP Cu samples. It is clear from Fig. 3a that the grains of the FSP-1 Cu sample were equiaxed and most grain boundaries were sharp, clear, and relatively straight with clear contrasts between neighboring grains, indicating that they were the grain boundaries with higher misorientation angles [5,21]. Many straight boundaries that traversed the whole grains were frequently observed in the fine grains, as illustrated by the arrows in Fig. 3a. According to the typical selected-area electron diffraction pattern shown in the upper right corner, most of them were $\Sigma 3$ coincident-site lattice twin boundaries (TBs). One typical characteristic of the FSP materials is the recrystallized microstructure [15–20]. Therefore, these TBs in Fig. 3a should be annealing TBs which formed during the recrystallization process. From the typical high-resolution TEM image in Fig. 3b, it can be seen that these annealing TBs were

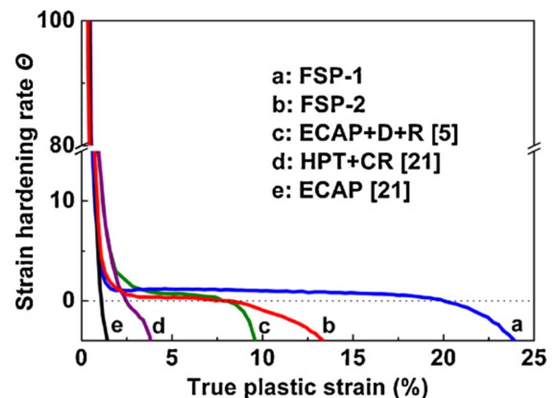

Fig. 2. Normalized strain hardening rate (Θ) against true stain of the UFG Cu prepared by FSP and SPD methods [5,21].

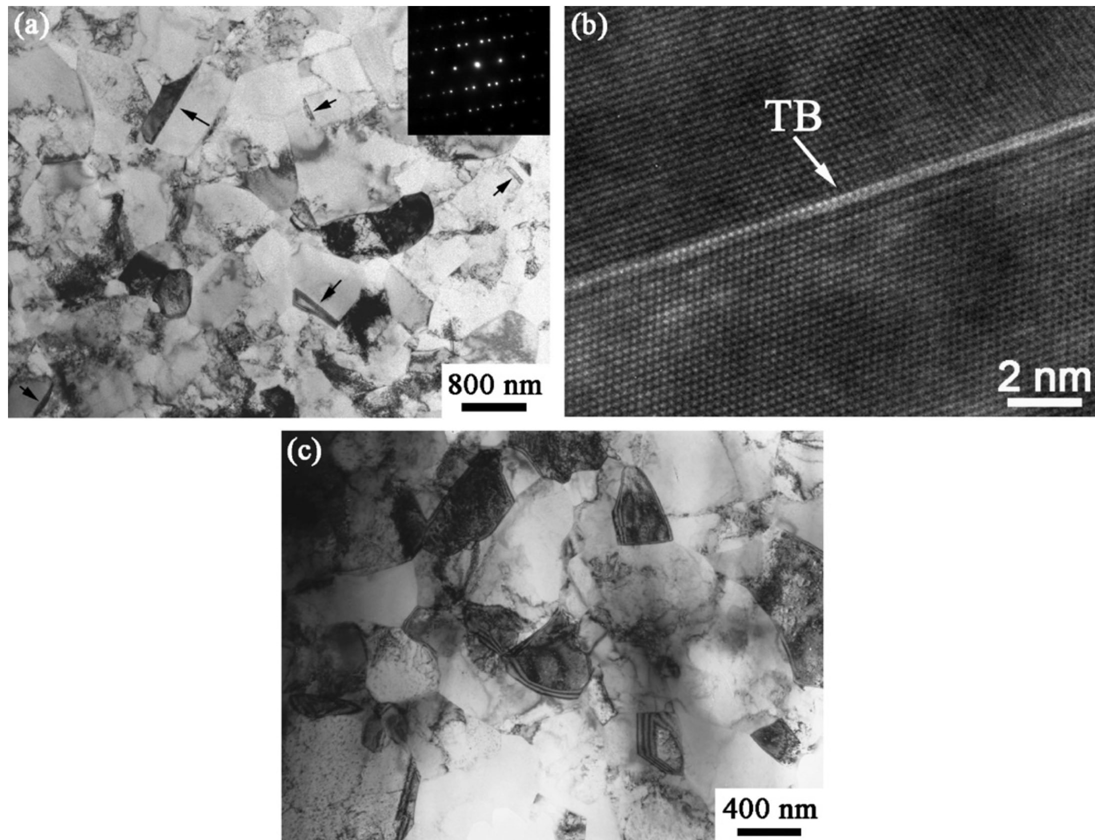

Fig. 3. (a) Typical bright-field (BF) TEM image of FSP-1 Cu sample, inset: selected-area electron diffraction pattern of the TB, (b) high-resolution TEM image of the TB in FSP-1 Cu sample and (c) BF TEM image of FSP-2 sample.

perfectly coherent and no lattice dislocation was detected. The similar microstructure with reduced grain size and Σ3 TBs was also obtained in the FSP-2 Cu sample, as shown in Fig. 3b.

It is clear from the TEM observations that both FSP Cu samples exhibited recrystallized grain structure, therefore, the grain refinement in the FSP Cu samples referred to the dynamic recrystallize (DRX) mechanism. Many researchers have investigated the grain refinement mechanism of the FSP materials; however, there is still no consensus among their results [17–20,22]. Usually, three DRX mechanisms, continuous DRX (CDRX), discontinuous DRX (DDRX), geometric DRX (GDRX), have been invoked as the mechanisms for the development of FSP fine grained microstructures [22]. Furthermore, dynamic recovery (DRV) was also considered as the grain refinement mechanism in FSP Al alloys which had high stacking fault energies (SFEs) [19,22]. The FSP microstructure would undergo the growth stage of the grains after the formation of the initial grain units, so it is difficult to reveal the initial crystallites formation. Su et al. [20] found that the early elongated crystallites transformed quickly to equiaxed grain structures by stable coarsening after passage of the FSP tool.

DRX should be the refinement mechanism for the FSP Cu with relatively low SFE, and the final structure in the present FSP Cu samples consisted of the coarsened grains after the growth stage. Once a given volume of plastically deformed material was outside the deformation zone of the rotating tool pin, it coarsened very quickly under the influence of heat [19,20]. At lower heat input, the grain growth of the FSP-2 Cu sample was more strongly inhibited during DRX process compared to that of the FSP-1 Cu sample. Therefore, the smaller grain size was obtained in the FSP-2 Cu sample, but the number of TBs was reduced because many TBs would form during the grain growth process of DRX [23].

The TEM microstructural characteristics were further confirmed by EBSD studies. The microstructure of the FSP Cu samples was characterized by fine grains with a typical equiaxed recrystallized microstructure (Fig. 4a and b). The average grain sizes of the FSP-1 Cu sample and FSP-2 Cu sample were ∼700 nm and ∼400 nm, respectively, calculated automatically by the grain area determination method of the Channel 5 software. It is noted that the distributions of grain boundary misorientation angles of both FSP Cu samples were similar to that of the random distribution for a cubic polycrystalline, but the ECAP Cu sample exhibited the significant different distribution (Fig. 4c and d). Considering all grain boundaries with misorientation angles >2°, the HAGBs (misorientation angle >15°) comprised about 90% and 75% of the total GB length in the FSP-1 and FSP-2 Cu samples, respectively. The fractions of HAGBs in both FSP Cu samples were obviously larger than that in SPD Cu samples in which the fraction of HAGBs reached only ∼60% even after complex procedures [5,21,24]. Compared with the ECAP Cu and also the random distribution for a cubic polycrystalline, the FSP-1 Cu sample exhibited one large peak at approximately 60°, which resulted from the Σ3 TBs.

The strain hardening is very important for UFG materials because the onset of plastic instability (necking or shear localization) in tension is governed by the Considére criterion

$$\left(\frac{\partial\sigma}{\partial\varepsilon}\right)_{\dot{\varepsilon}} \le \sigma \quad (2)$$

The ultra-fine grains tend to lose the work hardening (left-hand side of Eq. (2)) quickly on deformation owing to their very low dislocation storage efficiency inside the tiny grains [5,7]. Such a high-strength material is therefore prone to plastic instability, severely limiting the desirable ductility [7].

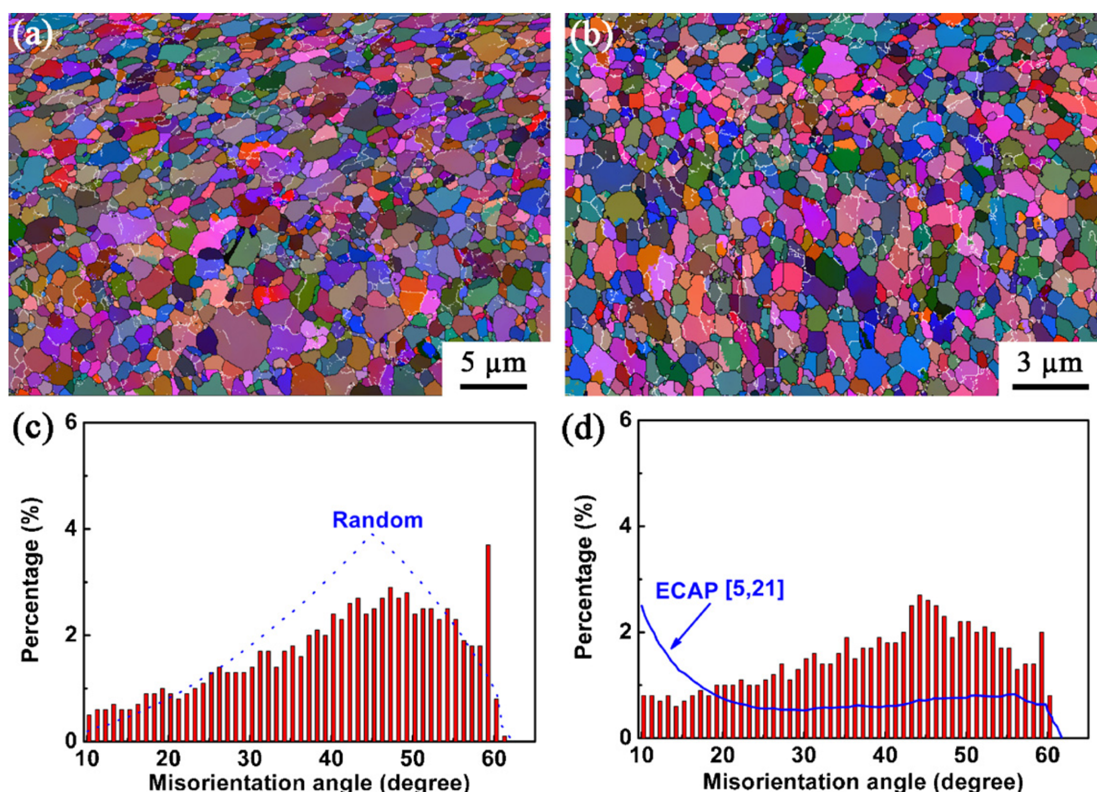

Fig. 4. Representative EBSD images of (a) FSP-1 Cu sample, (b) FSP-2 sample, and distribution of grain boundary misorientation angle for (c) FSP-1 Cu (the short dot line represents a random misorientation distribution for a cubic polycrystalline) and (d) FSP-2 Cu and 12-passes ECAP Cu [5,21].

Due to the DRV and DRX process during FSP, the dislocation density was very low in the FSP UFG materials [15–18]. Previous studies indicated that the tensile ductility could be enhanced in the UFG materials with lower dislocation density, which provided more room to store dislocations [8,21]. One of the structural features that often existed in UFG materials produced by SPD was their high dislocation density, which limited the further dislocation accumulation during tensile tests and the low strain hardening was usually achieved in this case [11–14]. Obviously, very low dislocation density in the present FSP Cu samples due to the DRX process resulted in the enhanced strain hardening capacity. The low dislocation density allowed further dislocation accumulation during tensile tests, and this led to the strain hardening.

Earlier reports demonstrated that coherent growth TBs usually exhibited high capacity to accommodate dislocations due to their much higher thermal and mechanical stability [6,25]. Copious TBs could be formed in the UFG materials produced via SPD methods, however, most of them were deformation TBs [5,12,25]. High density of partial dislocations existed along these deformation TBs, of which the excess energy was higher than that of fully coherent TBs [25]. These deformation TBs had little dislocation storage capacity, so the ductility increased by these TBs was limited [5,12]. However, as mentioned before, the TBs in the FSP Cu samples were coherent annealing TBs, which differed structurally from the deformation TBs. Moreover, the TBs tended to be distributed in the finer grains (Fig. 3a), which was attributed to that the stable TBs inhibited the further grain growth during recrystallization process [23]. It is believed that some strain hardening might be obtained in the fine grains owing to the existence of the coherent annealing TBs in the present FSP Cu samples.

One significant characteristic of the present FSP Cu samples was the large fraction of HAGBs as a result of recrystallization. Besides the intrinsic dislocations which formed the GBs, few dislocations existed near these HAGBs (Fig. 3a). So these HAGBs were different from the wavy, diffuse, and ill-defined non-equilibrium GBs resulting from SPD [5,21,26]. Non-equilibrium GBs in the SPD UFG materials contained a large number of extrinsic dislocations and represent the source of long-range internal stress [26]. It is believed that the HAGBs were more effective in accumulating slipping dislocations than low angle grain boundaries (LAGBs) [5,8,21]. Slipping dislocations was probably easier to react with the extrinsic dislocations in the LAGBs and this would lead to an annihilation of dislocations and a near-zero dislocation accumulation [21]. By contrast, the HAGBs in the present FSP Cu samples had few extrinsic dislocations, so they were more effective in blocking slipping dislocations, thereby forcing more dislocations to tangle and accumulate near the boundaries.

On the other hand, though the detailed mechanism was still not fully understood, some trials indicated that reasonable ductility could be enhanced by the HAGB sliding and related activities in UFG materials [8,27]. In the present FSP Cu samples, obvious large fraction of HAGBs was obtained, so HAGB sliding and related activities might generate, especially in the finer grain structure of the FSP-2 Cu sample. Fig. 5 shows the fracture surface of the FSP-2 Cu sample after tensile test. It is obvious that relatively flat zone could be observed besides the dimple zone which is the typical fracture characteristic for Cu (Fig. 5a). From the magnified micrograph (Fig. 5b), the flat zone was characterized by hummock-like features, and the size of the hummock was similar to the grain size of the FSP-2 Cu sample. That is to say, HAGB sliding and related activities were very likely to happen for the ultrafine grains in the FSP Cu samples during tensile deformation. The in-depth examination is in progress to elucidate the detailed mechanism of HAGB sliding. HAGB sliding led to dislocation emissions at the triple junctions of the grains owing to the presence of high stress concentrations, and these dislocations might act to

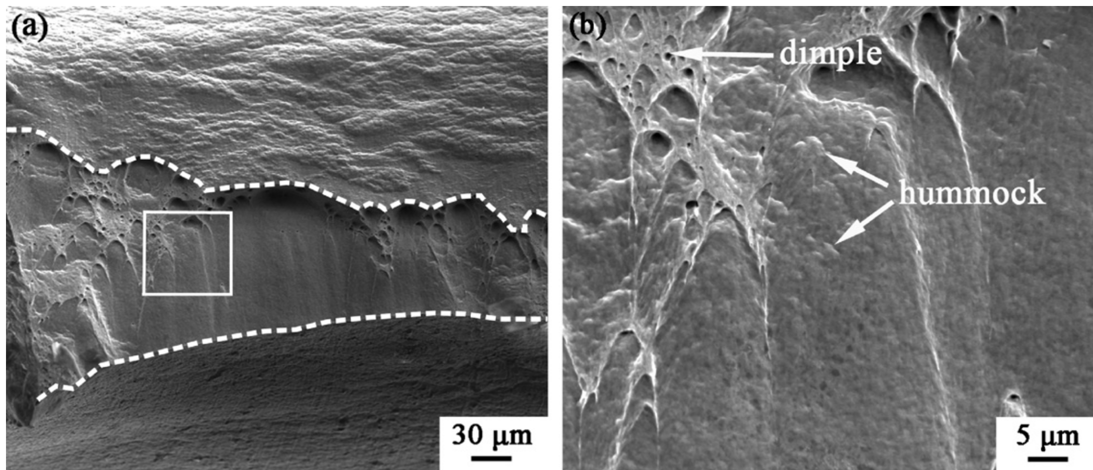

Fig. 5. (a) Fractograph of FSP-2 Cu after tensile test and (b) magnified review of the area as shown by the rectangle in Fig. 5(a).

increase the strain hardening [5,8]. Therefore, a large fraction of HAGBs could increase the strength and strain hardening simultaneously.

4. Conclusions

In summary, the following conclusions are reached:

1. UFG pure copper with high strength/ductility was successfully prepared by FSP. The YS and elongation were ~300 MPa and ~35% for the FSP-1 Cu sample with a grain size of ~700 nm, and ~370 MPa and ~22% for the FSP-2 Cu sample with a grain size of ~400 nm, respectively. Further, both FSP Cu samples showed continuous strain hardening to significant strains.
2. The microstructure of the FSP Cu samples was characterized by equiaxed grains with low dislocation density and predominant HAGBs as high as ~90% in the FSP-1 Cu sample. Furthermore, many annealing TBs were frequently observed in the fine grains.
3. The sound tensile properties of the FSP Cu samples were attributed to the enhanced strain hardening capacity in the special microstructure, where the dislocations could be accumulated effectively.

Acknowledgments

This work was supported by the National Natural Science Foundation of China under Grants No. 50890171 and No. 51071150, the National Basic Research Program of China under Grant No. 2011CB606301, and the National Outstanding Young Scientist Foundation under Grant No. 50525103.

References

[1] M. Dao, L. Lu, R.J. Asaro, J.T.M. De Hosson, E. Ma, Acta Mater. 55 (2007) 4041–4065.
[2] C.C. Koch, D.G. Morris, K. Lu, A. Inoue, MRS Bull. 24 (1999) 54–58.
[3] C.C. Koch, Scr. Mater. 49 (2003) 657–662.
[4] Y.T. Zhu, X.Z. Liao, Nat. Mater. 3 (2004) 351–352.
[5] Y.H. Zhao, J.F. Bingert, X.Z. Liao, B.Z. Cui, K. Han, A.V. Sergueeva, A.K. Mukherjee, R.Z. Valiev, T.G. Langdon, Y.T. Zhu, Adv. Mater. 18 (2006) 2949–2953.
[6] L. Lu, Y.F. Shen, X.H. Chen, L.H. Qian, K. Lu, Science 304 (2004) 422–426.
[7] Y.M. Wang, M.W. Chen, F.H. Zhou, E. Ma, Nature 419 (2002) 912–914.
[8] Y.H. Zhao, Y.T. Zhu, E.J. Lavernia, Adv. Eng. Mater. 12 (2010) 769–778.
[9] K.M. Youssef, R.O. Scattergood, K.L. Murty, J.A. Horton, C.C. Koch, Appl. Phys. Lett. 87 (2005) 091904.
[10] R. Valiev, Nat. Mater. 3 (2004) 511–516.
[11] F.D. Torre, R. Lapovok, J. Sandlin, P.F. Thomson, C.H.J. Davies, E.V. Pereloma, Acta Mater. 52 (2004) 4819–4832.
[12] W.S. Zhao, N.R. Tao, J.Y. Guo, Q.H. Lu, K. Lu, Scr. Mater. 53 (2005) 745–749.
[13] Y.M. Wang, E. Ma, M.W. Chen, Appl. Phys. Lett. 80 (2002) 2395–2397.
[14] A.P. Zhilyaev, T.G. Langdon, Prog. Mater. Sci. 53 (2008) 893–979.
[15] R.S. Mishra, M.W. Mahoney, S.X. McFadden, N.A. Mara, A.K. Mukherjee, Scr. Mater. 42 (1999) 163–168.
[16] R.S. Mishra, Z.Y. Ma, Mater. Sci. Eng. R 50 (2005) 1–78.
[17] J.Q. Su, T.W. Nelson, C.J. Sterling, Scr. Mater. 52 (2005) 135–140.
[18] C.I. Chang, X.H. Du, J.C. Huang, Scr. Mater. 57 (2007) 209–212.
[19] N. Kumar, R.S. Mishra, C.S. Huskamp, K.K. Sankaran, Mater. Sci. Eng. A 528 (2011) 5883–5887.
[20] J.Q. Su, T.W. Nelson, T.R. McNelley, R.S. Mishra, Mater. Sci. Eng. A 528 (2011) 5458–5464.
[21] Y.H. Zhao, J.F. Bingert, Y.T. Zhu, X.Z. Liao, R.Z. Valiev, Z. Horita, T.G. Langdon, Y.Z. Zhou, E.J. Lavernia, Appl. Phys. Lett. 92 (2008) 081903.
[22] T.R. McNelley, S. Swaminathan, J.Q. Su, Scr. Mater. 58 (2008) 349–354.
[23] P. Xue, G.M. Xie, B.L. Xiao, Z.Y. Ma, L. Geng, Metall. Mater. Trans. A 41 (2010) 2010–2021.
[24] C.X. Huang, H.J. Yang, S.D. Wu, Z.F. Zhang, Mater. Sci. Forum 584-586 (2008) 333–337.
[25] K. Lu, L. Lu, S. Suresh, Science 324 (2009) 349–352.
[26] R.Z. Valiev, R.K. Islamgaliev, I.V. Alexandrov, Prog. Mater. Sci. 45 (2000) 103–189.
[27] N.Q. Chinh, P. Szommer, Z. Horita, T.G. Langdon, Adv. Mater. 18 (2006) 34–39.